The Effect of Intermetallic Compound Morphology on Cu Diffusion in Sn-Ag and Sn-Pb Solder Bump on the Ni/Cu Under-Bump Metallization

GUH-YAW JANG[1] and JENQ-GONG DUH[1,2]

1.—Department of Materials Science and Engineering, National Tsing Hua University, Hsinchu 300, Taiwan. 2.—E-mail: jgd@mx.nthu.edu.tw

The eutectic Sn-Ag solder alloy is one of the candidates for the Pb-free solder, and Sn-Pb solder alloys are still widely used in today's electronic packages. In this study, the interfacial reaction in the eutectic Sn-Ag and Sn-Pb solder joints was investigated with an assembly of a solder/Ni/Cu/Ti/Si_3N_4/Si multilayer structures. In the Sn-3.5Ag solder joints reflowed at 260°C, only the $(Ni_{1-x},Cu_x)_3Sn_4$ intermetallic compound (IMC) formed at the solder/Ni interface. For the Sn-37Pb solder reflowed at 225°C for one to ten cycles, only the $(Ni_{1-x},Cu_x)_3Sn_4$ IMC formed between the solder and the Ni/Cu under-bump metallization (UBM). Nevertheless, the $(Cu_{1-y},Ni_y)_6Sn_5$ IMC was observed in joints reflowed at 245°C after five cycles and at 265°C after three cycles. With the aid of microstructure evolution, quantitative analysis, and elemental distribution between the solder and Ni/Cu UBM, it was revealed that Cu content in the solder near the solder/IMC interface played an important role in the formation of the $(Cu_{1-y},Ni_y)_6Sn_5$ IMC. In addition, the diffusion behavior of Cu in eutectic Sn-Ag and Sn-Pb solders with the Ni/Cu UBM were probed and discussed. The atomic flux of Cu diffused through Ni was evaluated by detailed quantitative analysis in an electron probe microanalyzer (EPMA). During reflow, the atomic flux of Cu was on the order of 10^{16}–10^{17} atoms/cm^{2}sec in both the eutectic Sn-Ag and Sn-Pb systems.

Key words: Flip chip, Sn-Ag solder, Sn-Pb solder, diffusion, intermetallic compound (IMC), under-bump metallization (UBM)

INTRODUCTION

The Sn-Pb solder is widely used in today's electronic package. Nevertheless, because of the toxic effect of Pb on human beings and the environment, several Pb-free solders have been investigated to replace the Sn-Pb solder.[1–4] The eutectic Sn-Ag solder is one of the candidates because of its excellent mechanical properties.[5] Flip-chip technology (FCT) has been used since the 1960s[6] and exhibits several advantages, such as high input/output connects, high-frequency performance, and easy assembly. It has thus become one of the most attractive processing methods in microelectronics.[7,8] One of the challenging issues is the material selection for under-bump metallization (UBM). The Ni-based UBM is of interest in FCT because of the low growth rate of the Ni-Sn compound and limited spalling effect.[9,10] The Cu metallization possesses excellent electrical properties and is widely used as interconnects in FCT.[11]

Recently, the effect of reflow times on the interfacial reactions between the solder and Ni/Cu UBM in the SnAg and SnPb systems was reported.[12,13] The phase transformation of intermetallic compounds (IMCs) and Cu diffusion on the interfacial reaction in the SnPb solder joints were also discussed.[14,15] The literature concerning the effect of reflow temperature on the interfacial reactions and Cu diffusion between the Sn-Pb solder and Ni/Cu is, however, limited. The objectives of this study were first to investigate the detailed interfacial reactions between Sn-Ag, Sn-Pb solders, and the Ni/Cu UBM at

(Received March 13, 2004; accepted August 30, 2004)

different reflow temperatures. The diffusion behavior of Cu between solders and the Ni/Cu UBM in both Sn-Ag and Sn-Pb systems was discussed. Assemblies of Sn-3.5Ag/Ni/Cu/Ti/Si_3N_4/Si and Sn-37Pb/Ni/Cu/Ti/Si_3N_4/Si multilayer structures were used. Titanium played the role of the adhesion layer, Cu was the conductor, while Ni acted as the wetting layer and diffusion barrier. The Sn-3.5Ag and Sn-37Pb solder joints followed by multiple reflows were employed for microstructural evaluation of IMCs. After analyzing the concentration profiles of Cu in Sn-3.5Ag and Sn-37Pb joints after reflows, the diffusion behavior of Cu was revealed. In addition, the correlation between Cu contents in the solder near the solder/IMC interface and IMC formation were investigated and discussed.

EXPERIMENTAL PROCEDURES

Two different solder alloys were used in this study: one was the lead-free Sn-3.5Ag solder and the other was the eutectic Sn-37Pb solder. For the UBM structure used, the top metal of the Si wafer was Cu, which acted as an interconnection line. The adhesion layer was sputtered Ti of 1,000 Å. For the electroplated seed layer, 5,000-Å Cu was then sputtered on Ti. The electroplated Cu with 5-μm thickness was further deposited on the metallized substrate. A 3.5-μm Ni layer was electroplated on the top of the electroplated Cu to be jointed with the solder bump. After the UBM was plated onto the Si wafer, the solder bumps were then electroplated. All metal films were deposited consecutively without breaking vacuum.

Solder reflows were conducted in a solder reflow oven (Falcon 5 × 5 Multi-Purpose System, SIKAMA, Santa Barbara, CA). The peak temperature of the reflow profile for Sn-Ag bumps was set at 260°C, and dwelling time was 100 sec. On the other hand, three kinds of reflow profiles for Sn-Pb bumps were chosen, and the peak temperatures of the reflow profile were 225°C, 245°C, and 265°C, respectively. The dwelling times were 116 sec, 124 sec, and 120 sec for reflow at 225°C, 245°C, and 265°C, respectively. The cycles of solder reflow were from one to ten times.

For the cross-sectional analysis, the Si dies were cold-mounted in epoxy, sectioned using a slow-speed diamond saw, ground, polished, and etched. For the top-view samples, the solder balls were etched directly with one part nitric acid, one part acetic acid, and four parts glycerin at 80°C. The morphologies of interfacial products between solders and the UBM were analyzed with field-emission scanning electron microscopy (FESEM, JSM-6500F, JEOL, Japan Electron Optics Laboratory, Tokyo). The compositions of phases in the solder joints and elemental distribution across the joint interface were quantitatively measured with an electron probe microanalyzer (EPMA, JXA-8800M, JEOL) with the aid of a ZAF program.[16]

RESULTS AND DISCUSSION

Interfacial Reaction between the Sn-3.5Ag Solder and UBM during Multiple Reflows

Figure 1 shows the cross-sectional images of the interface between the Sn-3.5Ag solder and Ni/Cu UBM after one, four, and ten reflows. Only one type of interfacial product was found between the solder and Ni metallization. The size of the reaction product formed in the Sn-3.5Ag joint after one reflow is close to the detection limit of the EPMA if the resolution of the electron probe size is considered. To obtain reliable quantitative data, a deliberative task was carefully employed in the EPMA analysis by choosing the appropriate accelerating voltage, beam current, and focus-beam size. The reported compositions as listed in this study were the average of at least ten measured points. The average composition of the interfacial product was 56.9at.%Sn, 1.8at.%Cu, and 41.3at.%Ni in the Sn-3.5Ag joint after one reflow. The atomic ratio of (Ni + Cu) to Sn was (41.3 + 1.8):56.9, which is close to 3:4. Thus, the interfacial product could be denoted as $(Ni_{1-x},Cu_x)_3Sn_4$. After four and ten reflows, the Cu concentration in the $(Ni_{1-x},Cu_x)_3Sn_4$ IMC decreased slightly from the $(Ni_{1-x},Cu_x)_3Sn_4$/Ni interface toward the solder/$(Ni_{1-x},Cu_x)_3Sn_4$ one, as indicated in Table I and Fig. 1.

After the first reflow cycle, the scalloped-type $(Ni_{1-x},Cu_x)_3Sn_4$ IMC exhibited a rather round inter-

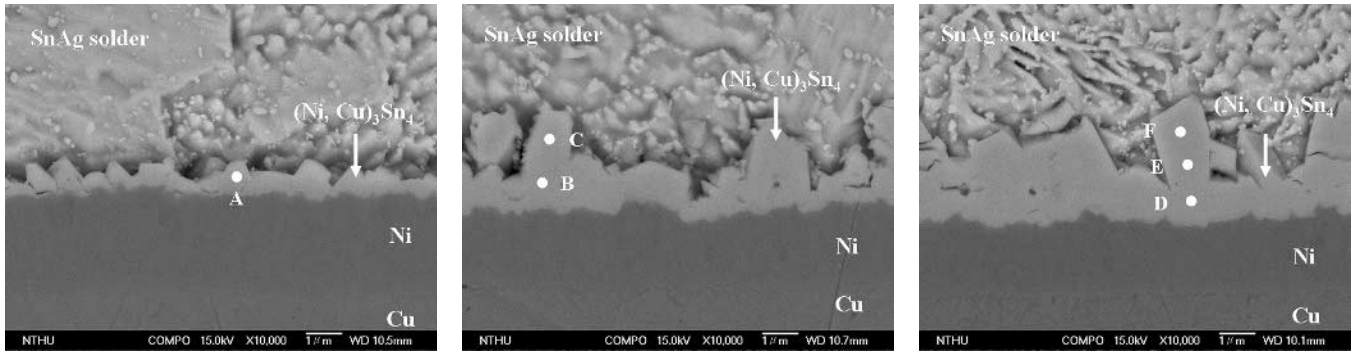

a b c

Fig. 1. Cross-sectional images of interfacial morphology in Sn-3.5Ag solder/Ni/Cu joints during various reflows: (a) one, (b) four, and (c) ten cycles.

Table I. Quantitative Analysis Results for Trace Points in Fig. 1 in the Sn-3.5Ag Solder Joints

Measurement Locations	Composition (at.%) Ni	Cu	Sn	Phase
A	41.1	1.7	57.2	$(Ni_{1-x},Cu_x)_3Sn_4$
B	41.1	1.9	57.0	$(Ni_{1-x},Cu_x)_3Sn_4$
C	41.5	1.5	57.0	$(Ni_{1-x},Cu_x)_3Sn_4$
D	40.9	2.3	56.8	$(Ni_{1-x},Cu_x)_3Sn_4$
E	41.4	1.8	56.8	$(Ni_{1-x},Cu_x)_3Sn_4$
F	41.6	1.4	57.0	$(Ni_{1-x},Cu_x)_3Sn_4$

face. However, with increasing reflows, the interface between the solder and the Ni layer became wavy (Fig. 1). For example, the nodule size of the $(Ni_{1-x},Cu_x)_3Sn_4$ IMC formed after one reflow was less than 1 μm. After ten reflows, a larger size of nodules, 2–4 μm in diameter, could be observed between the solders and Ni. Figure 2 exhibits the thickness of the $(Ni_{1-x},Cu_x)_3Sn_4$ IMC in the Sn-3.5Ag solder joints after one, four, and ten reflows. It is clearly indicated that the $(Ni_{1-x},Cu_x)_3Sn_4$ IMC in the Sn-3.5Ag solder joints grew gradually during reflow. Figure 3 shows the top-view micrographs of the IMC in the Sn-Ag system after one, four, and ten reflows. Those $(Ni_{1-x},Cu_x)_3Sn_4$ IMCs exhibited a faceted and particle-like morphology. The grain sizes of the $(Ni_{1-x},Cu_x)_3Sn_4$ IMC formed after one, four, and ten reflows are 0.6– 1.5 μm, 1.4–3.5 μm, and 1.5–5.0 μm, respectively. Statistically speaking, the grain size distribution of the $(Ni_{1-x},Cu_x)_3Sn_4$ IMC formed after ten reflows was broader than that formed after one reflow. As a result, a wavy interface was revealed between the solders and UBM after ten reflows.

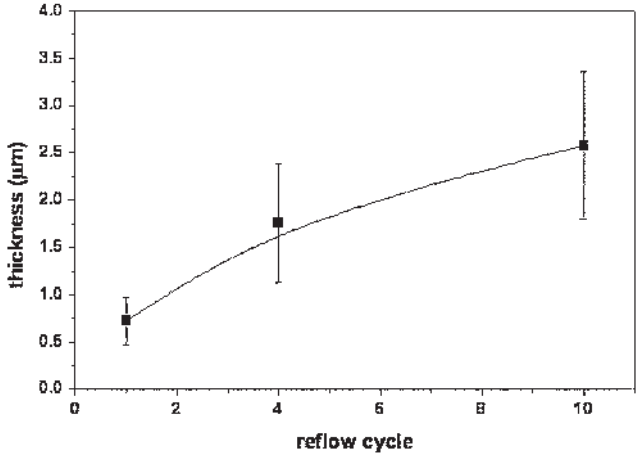

Fig. 2. The thickness of the $(Ni_{1-x},Cu_x)_3Sn_4$ IMC formed in the Sn-3.5Ag/Ni/Cu joints after multiple reflows.

Interfacial Reaction between the Sn-37Pb Solder and UBM during Multiple Reflows

The Sn-37Pb/Ni/Cu Joints Reflowed at 225°C

Figure 4 exhibits the cross-sectional images of interfacial morphology in the Sn-37Pb joints reflowed at 225°C for one and ten cycles. Only one scalloped-type interfacial product was observed at the Sn-37Pb solder/Ni interface in the joints reflowed at 225°C for one, three, five, and ten cycles. In the joint after ten reflows, the thickness and composition of the scalloped-type product was 1.16 ± 0.37 μm, and the measured composition of was 56.7at.%Sn, 40.0at.%Ni, and 3.3at.%Cu. The ratio of the atomic percentage of (Ni + Cu) to Sn was (40.0 + 3.3): (56.7), which is close to 3:4. Thus, the scalloped-type reaction product could be denoted as the $(Ni_{1-x},Cu_x)_3Sn_4$ IMC. The value of x in the $(Ni_{1-x},Cu_x)_3Sn_4$ IMC maintain around 0.08 for the joints reflowed at 225°C for one to ten cycles, as shown in Table II. In addition, the thickness of the $(Ni_{1-x},Cu_x)_3Sn_4$ IMC was 0.68 ± 0.12, 0.75 ± 0.25, 1.09 ± 0.34, and 1.16 ± 0.37 in the joints reflowed for one, three, five, and ten cycles, respectively, as shown in Fig. 5. It is clearly indicated that the $(Ni_{1-x},Cu_x)_3Sn_4$ IMC in the joints reflowed at 225°C grew gradually with increasing reflow cycles.

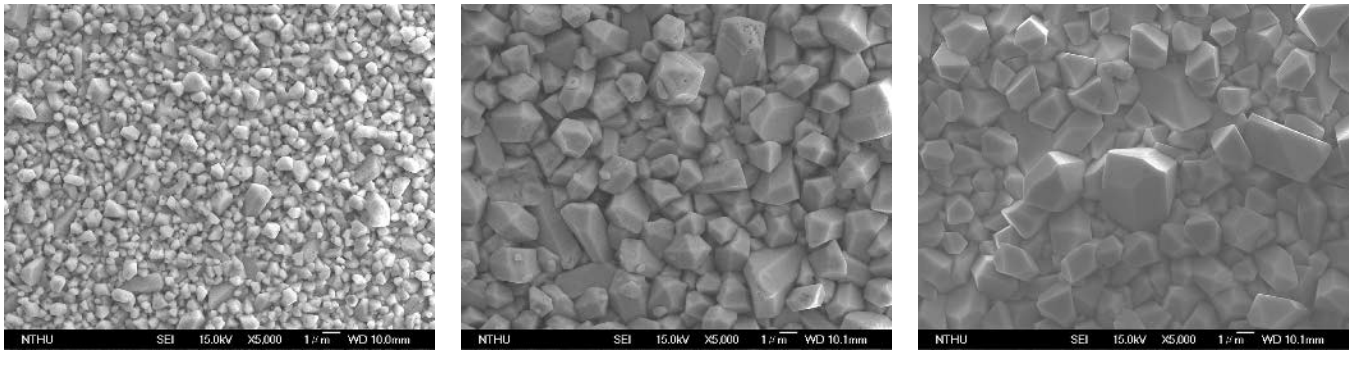

a b c

Fig. 3. Top-view morphology of the $(Ni_{1-x},Cu_x)_3Sn_4$ IMC in Sn-3.5Ag solder/Ni/Cu joints during various reflows: (a) one, (b) four, and (c) ten cycles.

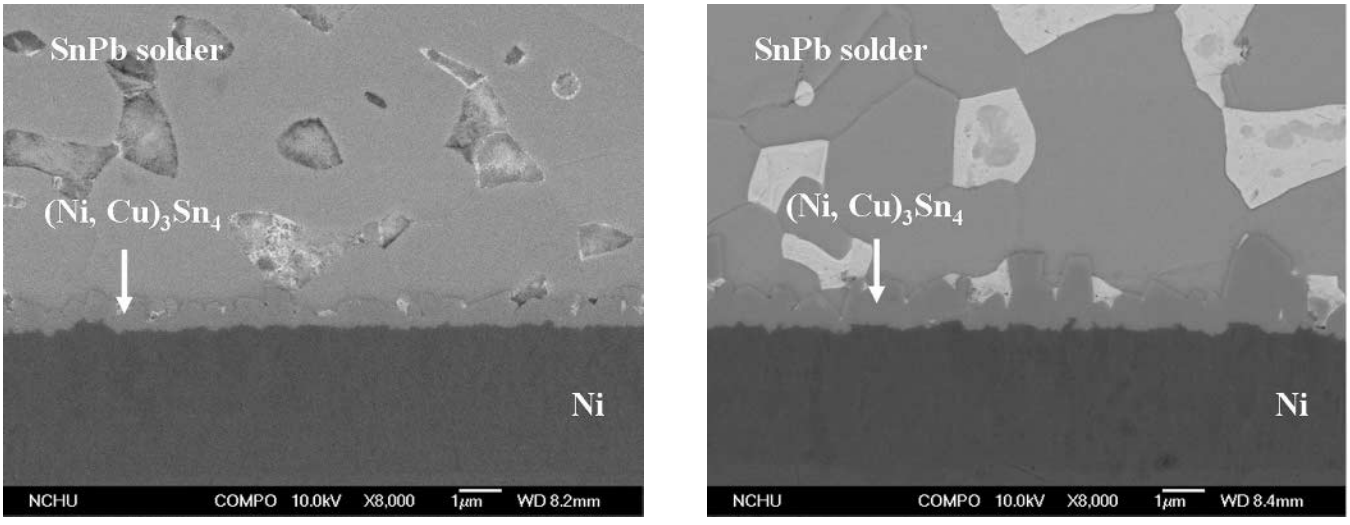

a b

Fig. 4. Cross-sectional images of interfacial morphology in the Sn-37Pb solder/Ni/Cu joints reflowed at 225°C for (a) one and (b) ten cycles.

Table II. Composition of IMCs Formed in the Sn-37Pb/Ni/Cu Joints at Various Reflow Temperatures after Multiple Reflows

Peak Temperature	Reflow Cycles	$(Ni_{1-x},Cu_x)_3Sn_4$	$(Cu_{1-y},Ni_y)_6Sn_5$
225°C	1, 3, 5, 10	x = 0.08	—
245°C	1, 3	x = 0.08	—
	5, 10	x = 0.08–0.22	y = 0.25–0.43
265°C	1	x = 0.08	—
	3, 5, 10	x = 0.08–0.24	y = 0.31–0.48

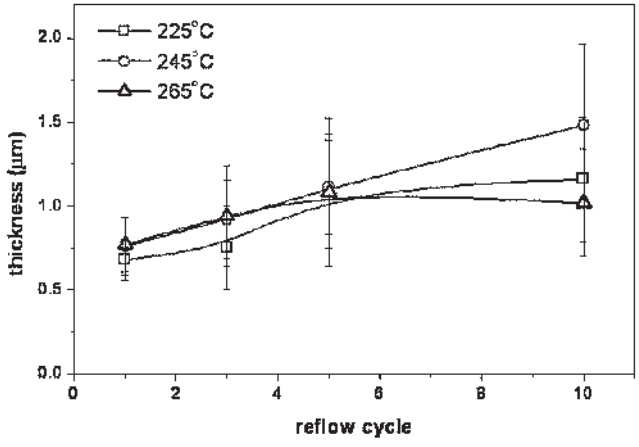

Fig. 5. The thickness of the $(Ni_{1-x},Cu_x)_3Sn_4$ IMC formed in the Sn-37Pb/Ni/Cu joints reflowed at 225°C, 245°C, and 265°C for various cycles.

To investigate the morphologies of the $(Ni_{1-x},Cu_x)_3Sn_4$ IMC more clearly, an etching solution was employed to remove the bulk solder. Figure 6 shows the top-view micrographs of the $(Ni_{1-x},Cu_x)_3Sn_4$ IMC in the Sn-37Pb joint reflowed at 225°C for one and ten cycles. The $(Ni_{1-x},Cu_x)_3Sn_4$ IMC exhibited a faceted and particle-like morphology. A combination of the cross-sectional images in Fig. 4 as well as the top-view morphology demonstrated in Fig. 6 showed that the grain sizes of the $(Ni_{1-x},Cu_x)_3Sn_4$ IMC increased with increasing reflow cycles. Statistically, the grain-size distribution of the $(Ni_{1-x},Cu_x)_3Sn_4$ IMC formed after ten reflows was broader than that after one reflow (Fig. 6). In fact, the grain size of the IMC formed after one, three, five, and ten reflows was 0.23–0.53 μm, 0.33–0.81 μm, 0.41–0.86 μm, and 0.69–1.28 μm, respectively. It is revealed from both cross-sectional and top-view images of the solder/Ni interface that the growth of the $(Ni_{1-x},Cu_x)_3Sn_4$ IMC was enhanced with increasing reflows.

The Sn-37Pb/Ni/Cu Joints Reflowed at 245°C

After one and three reflows, only one scalloped-type reaction product formed at the Sn-37Pb solder/Ni interface. The Sn-37Pb joints reflowed at 245°C for three cycles are typically presented in Fig. 7a. After detailed composition analysis by EPMA, the reaction product was identified as $(Ni_{1-x},Cu_x)_3Sn_4$. During five and ten reflows, the other island-type reaction product was observed between the Sn-37Pb solder and the $(Ni_{1-x},Cu_x)_3Sn_4$ IMC. The composition of the island-type reaction product was 45.1at.%Sn, 36.9at.%Cu, and 18.0at.%Ni. The ratio of (Cu + Ni) to Sn was close to 6:5. Thus, the island-type reaction product could be denoted as the $(Cu_{1-y},Ni_y)_6Sn_5$ IMC. The values of x in the $(Ni_{1-x},Cu_x)_3Sn_4$ IMC remained around 0.08 in the joint after one and three reflows (Table II). However, after five and ten reflows, the compositions of

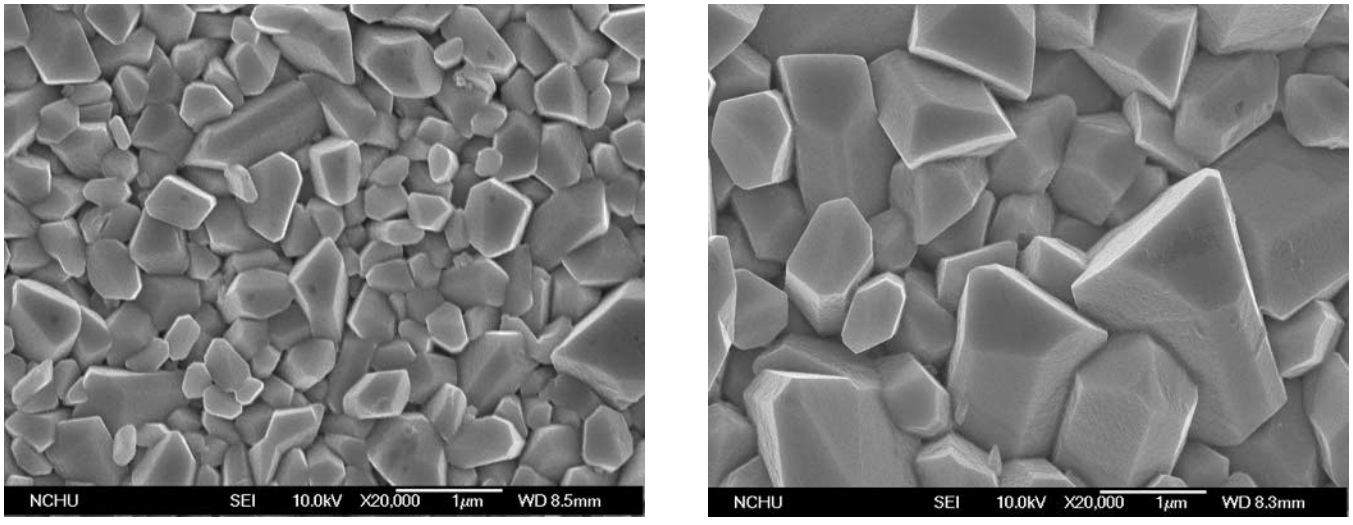

a b

Fig. 6. Top-view morphology of the $(Ni_{1-x},Cu_x)_3Sn_4$ IMC in the Sn-37Pb solder/Ni/Cu joints reflowed at 225°C for (a) one and (b) ten cycles.

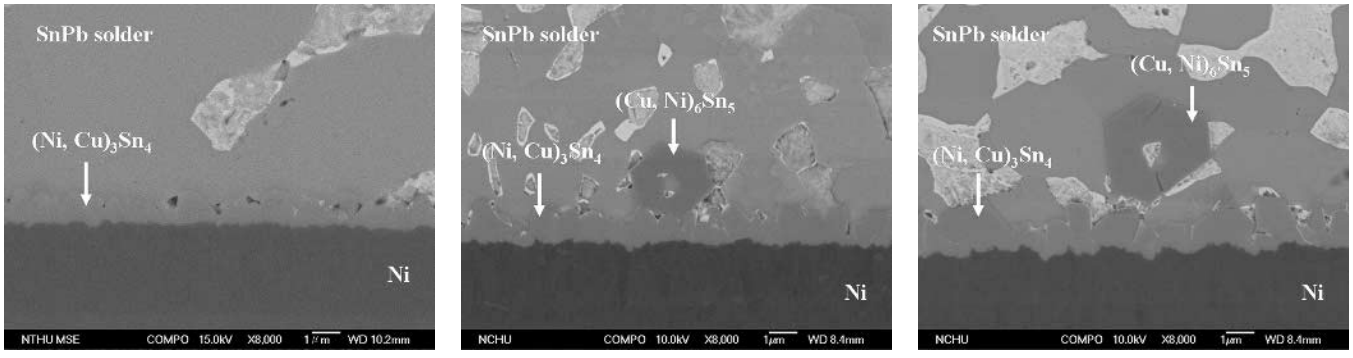

a b c

Fig. 7. Cross-sectional images of interfacial morphology in the Sn-37Pb solder/Ni/Cu joints reflowed at 245°C for (a) three, (b) five, and (c) ten cycles.

$(Ni_{1-x},Cu_x)_3Sn_4$ and $(Cu_{1-y},Ni_y)_6Sn_5$ IMCs were not fixed.

The top-view micrographs of IMCs in the Sn-37Pb joint reflowed at 245°C for three and ten cycles are illustrated in Fig. 8. The morphologies of the $(Ni_{1-x},Cu_x)_3Sn_4$ IMC after one and three reflows were faceted and particle-like, similar to that formed in the Sn-37Pb joint reflowed at 225°C. However, hexagonal-prism-type $(Cu_{1-y},Ni_y)_6Sn_5$ IMCs were revealed after five to ten reflows in the Sn-37Pb joint reflowed at 245°C (Fig. 8b). To calculate the volume of the $(Cu_{1-y},Ni_y)_6Sn_5$ IMC, it is assumed that the $(Cu_{1-y},Ni_y)_6Sn_5$ IMC was the perfect hexagonal prism, and consequently, the volume of the $(Cu_{1-y},Ni_y)_6Sn_5$ IMC can be expressed as

$$V_{Cu_6Sn_5} = \frac{\sqrt{3}}{2} a^2 (2\sqrt{b^2 - a^2} + 3c) \qquad (1)$$

where a indicates the base length of the prism, b is the side length of the prism, and c represents the long axial length of the hexagonal. The volume of the $(Cu_{1-y},Ni_y)_6Sn_5$ IMC after multiple reflows could be measured directly from the top-view images. Thus, the average thickness of the $(Cu_{1-y},Ni_y)_6Sn_5$ IMC was equivalent to the total volume of the $(Cu_{1-y},Ni_y)_6Sn_5$ IMC divided by the area of the pad.

The average thickness of the $(Cu_{1-y},Ni_y)_6Sn_5$ IMC in the Sn-37Pb joints reflowed at 245°C for five and ten cycles are 0.49 μm and 1.37 μm, as indicated in Fig. 9. It is clearly shown in Fig. 5 that the thickness of the $(Ni_{1-x},Cu_x)_3Sn_4$ IMC measured from cross-sectional images increases gradually with increasing reflows in the Sn-37Pb joints at 245°C. Thus, it was demonstrated that $(Ni_{1-x},Cu_x)_3Sn_4$ and $(Cu_{1-y},Ni_y)_6Sn_5$ IMCs in the Sn-37Pb joints reflowed at 245°C grew gradually with increasing reflows.

The Sn-37Pb/Ni/Cu Joints Reflowed at 265°C

For the joint reflowed at 265°C after one cycle, there was one reaction product at the Sn-37Pb solder/Ni interface. The scalloped-type product was identified as $(Ni_{1-x},Cu_x)_3Sn_4$ by quantitative analysis of the EPMA. The x value in the $(Ni_{1-x},Cu_x)_3Sn_4$ IMC in the joint reflowed at 265°C for one cycle was 0.8 and identical with that in the joint reflowed at 245°C for one and three cycles. After three, five, and ten reflows, the island-type $(Cu_{1-y},Ni_y)_6Sn_5$ IMC

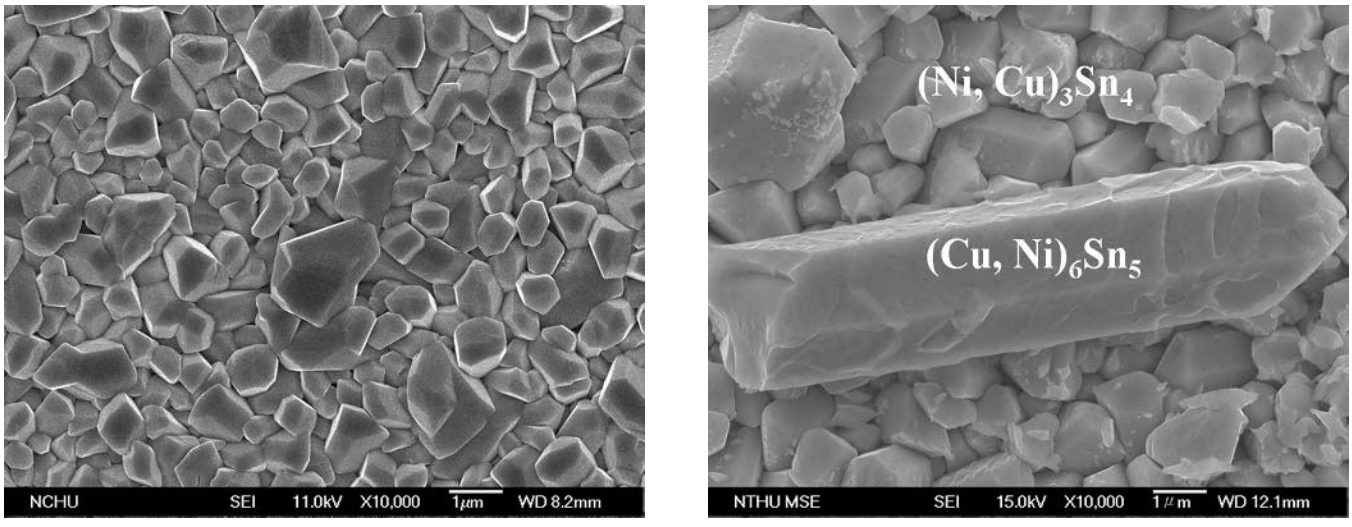

a b

Fig. 8. Top-view morphology of IMCs in the Sn-37Pb solder/Ni/Cu joints reflowed at 245°C for (a) three and (b) ten cycles.

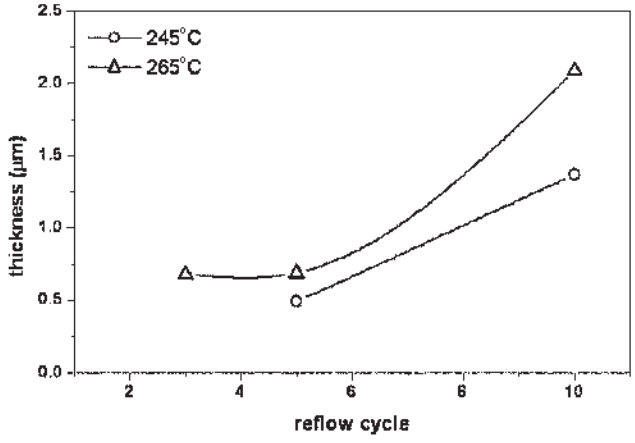

Fig. 9. The average thickness of the $(Cu_{1-y},Ni_y)_6Sn_5$ IMC formed in the Sn-37Pb/Ni/Cu joints reflowed at 245°C and 265°C for various cycles.

formed between the Sn-37Pb solder and the $(Ni_{1-x},Cu_x)_3Sn_4$ IMC, as shown in Fig. 10. The values of x in the $(Ni_{1-x},Cu_x)_3Sn_4$ IMC at 265°C during multiple reflows is altered between 0.08 and 0.24. On the other hand, the composition of the $(Cu_{1-y},Ni_y)_6Sn_5$ IMC in the joints reflowed at 265°C for various cycles was not fixed (Table II). In addition, the $(Cu_{1-y},Ni_y)_6Sn_5$ IMC grew gradually with increasing reflows in the Sn-37Pb joint at 265°C (Fig. 10). The thickness of the $(Ni_{1-x},Cu_x)_3Sn_4$ IMC in the Sn-37Pb joints reflowed at 265°C increased slowly until five reflows. After ten reflows, the thickness of the $(Ni_{1-x},Cu_x)_3Sn_4$ IMC was less than that after five reflows (Fig. 5). This implies that the growth of the $(Ni_{1-x},Cu_x)_3Sn_4$ IMC is decelerated and ever consumed after ten reflows. This will be further discussed later.

Figure 11 exhibits the top-view morphology of IMCs in the Sn-37Pb joints reflowed at 265°C for five and ten cycles. The morphologies of the $(Ni_{1-x},Cu_x)_3Sn_4$ IMC formed in the Sn-37Pb joints at 265°C during multiple reflows were faceted and particle-like, similar to that at both 225°C and 245°C. The size of $(Cu_{1-y},Ni_y)_6Sn_5$ IMCs reflowed at 265°C for ten cycles is much larger than that after five reflows (Fig. 11). Furthermore, it is apparently indicated in Fig. 9 that the $(Cu_{1-y},Ni_y)_6Sn_5$ IMC in the Sn-37Pb joint reflowed at 265°C for ten cycles is three times the average thickness of that after five reflows. This

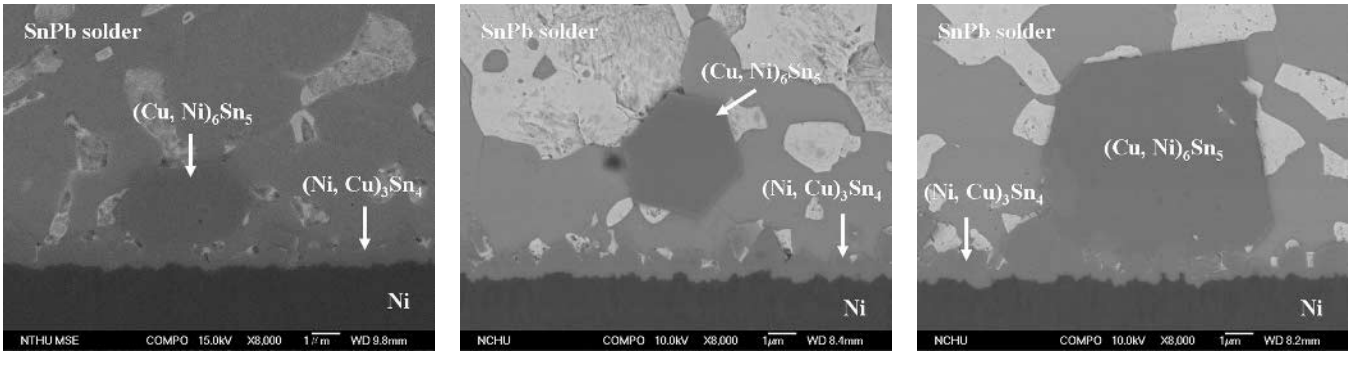

a b c

Fig. 10. Cross-sectional images of interfacial morphology in the Sn-37Pb solder/Ni/Cu joints reflowed at 265°C for (a) three, (b) five, and (c) ten cycles.

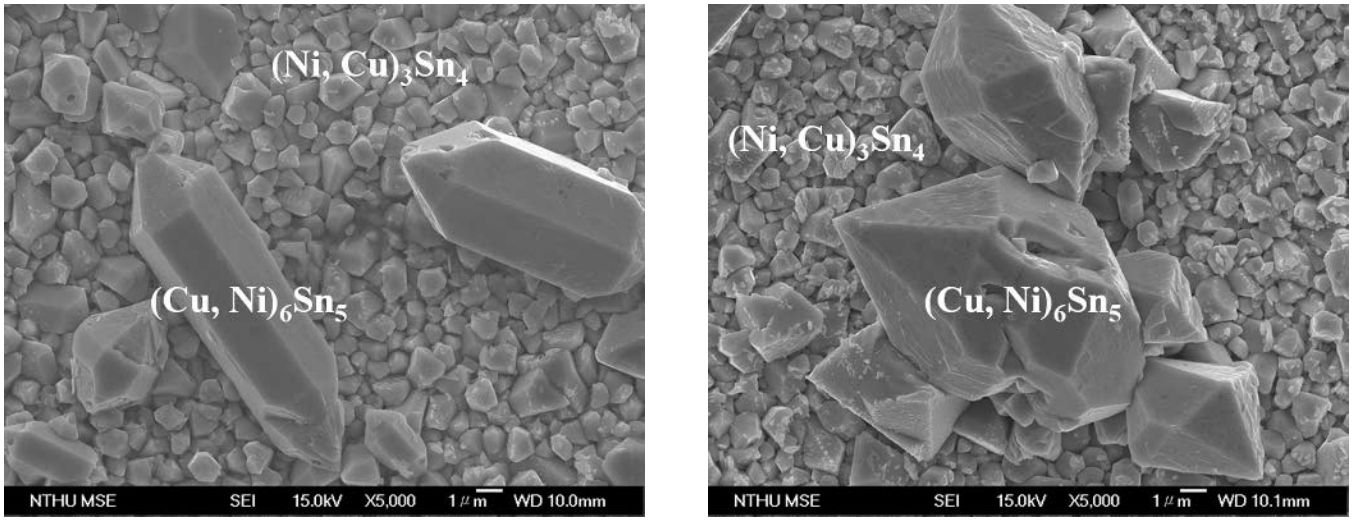

a b

Fig. 11. Top-view morphology of IMCs in the Sn-37Pb solder/Ni/Cu joints reflowed at 265°C for (a) five and (b) ten cycles.

demonstrates that the $(Cu_{1-y},Ni_y)_6Sn_5$ IMC at 265°C after five reflows grew rapidly.

The Atomic Flux of Cu in the Sn-3.5Ag and Sn-37Pb Joints after Multiple Reflows

The EPMA trace-line analyses across the Ni/IMC/solder interface, as indicated in Figs. 12b, 13b, and 14b, give evidence of the presence of Cu atoms in the Ni, IMC, and solder, respectively. The atomic flux of Cu, J_{Cu}, can be expressed as

$$J_{Cu}=\frac{(T_{IMC}C_{Cu\ in\ IMC}+T_{Ni}C_{Cu\ in\ Ni}+T_{solder}C_{Cu\ in\ solder})\rho_{Cu}N_0}{M_{Cu}t} \quad (2)$$

where T_i is the average thickness of i, $C_{Cu\ in\ i}$ is the concentration of Cu in i, ρ_{Cu} is the density of Cu, N_0

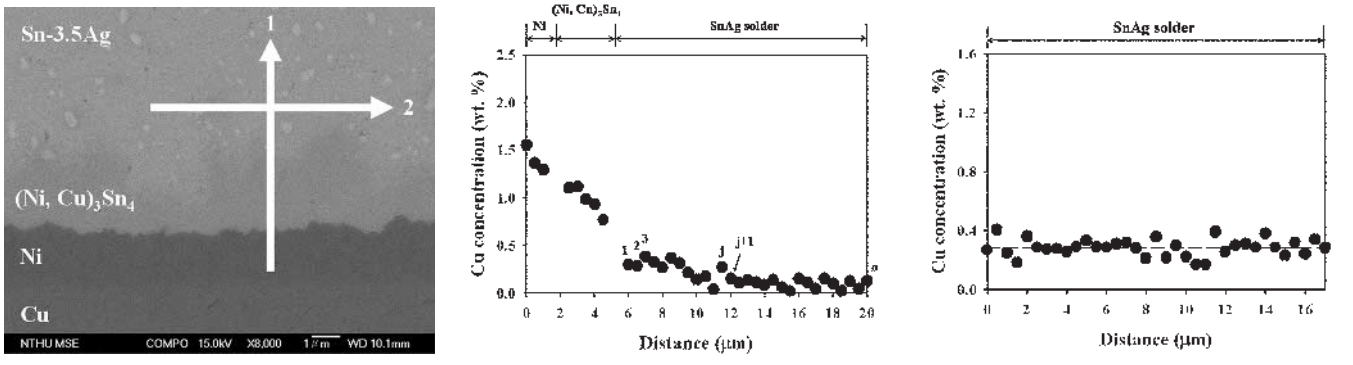

a b c

Fig. 12. (a) Cross-sectional image of Sn-3.5Ag solder/UBM interfaces in the joint after ten reflows, and the concentration profiles of Cu along (b) trace line 1 and (c) trace line 2 in (a).

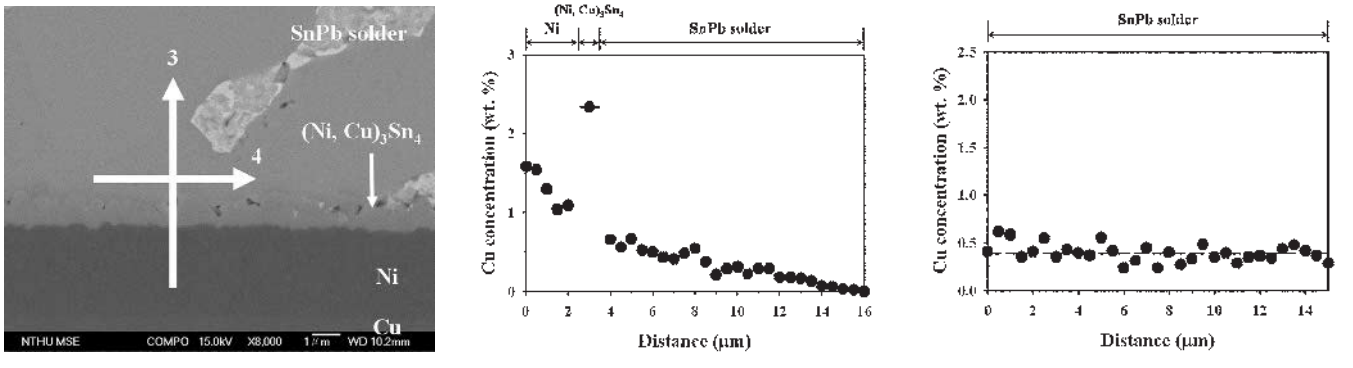

a b c

Fig. 13. (a) Cross-sectional image of the Sn-37Pb solder/UBM reflowed at 245°C for three cycles, and the concentration profiles of Cu along (b) trace line 3 and (c) trace line 4 in (a).

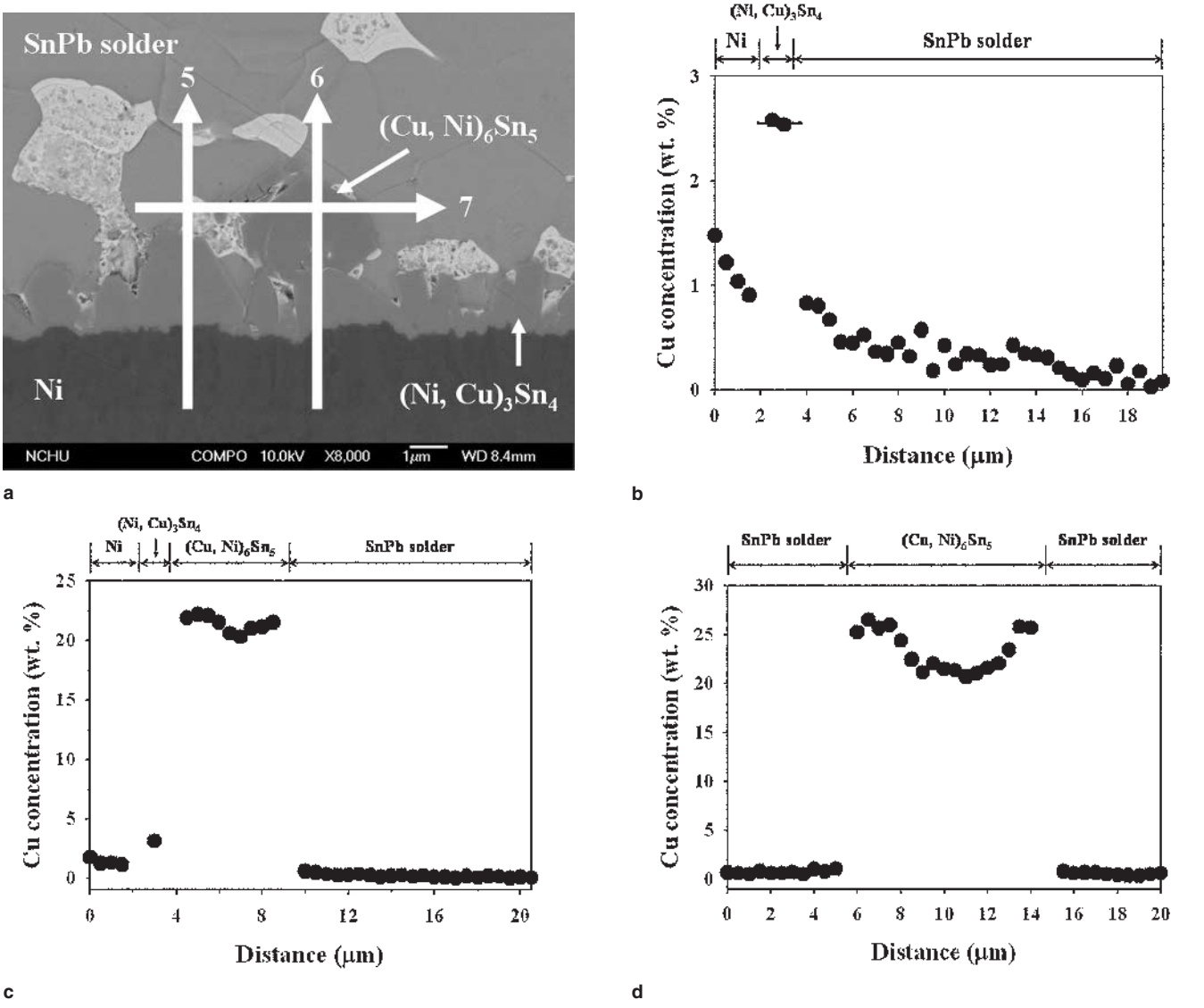

Fig. 14. (a) Cross-sectional image of the Sn-37Pb solder/UBM reflowed at 245°C for ten cycles, and the concentration profiles of Cu along (b) trace line 5, (c) trace line 6, and (d) trace line 7 in (a).

is Avogadro's number, M_{Cu} is the molecular weight of the Cu atom, and t is heat treatment time. In addition, the amount of diffused Cu atoms per joint, N_{Cu}, was calculated with Eq. 3:

$$N_{Cu} = J_{Cu} \times t \times \pi \times r^2 \quad (3)$$

where r is the radius of the solder pad and is equal 50 μm in this study. The Cu contents in the joints during reflows with respect to Ni metallization, IMCs, and solder, respectively, will be discussed. In addition, the atomic flux associated with Cu diffusion is also evaluated.

The Cu Content in Ni Metallization

The average thickness of unconsumed Ni and average concentration of Cu in the Ni metallization in the Sn-3.5Ag and Sn-37Pb joints during multiple reflows are listed in Table III. The thickness of the unconsumed Ni decreased slowly during reflow for all solder joints. In contrast with Sn-37Pb solder joints, the thickness of the unconsumed Ni in the Sn-3.5Ag solder joint was the thinnest in the case of ten reflows. For Sn-37Pb solder joints after ten reflows, the thickness of the unconsumed Ni reflowed at 245°C was greater than that reflowed at 265°C. It should be noted that the thickness of the Ni metallization after electrodeposition was 3.5 μm in both Sn-37Pb and Sn-3.5Ag solder joints. After ten reflows, the thickness of the reacted Ni in the Sn-37Pb was 0.77 μm and 0.85 μm for reflow at 245°C and 265°C, respectively, while it was 1.34 μm in the Sn-3.5Ag joint. This demonstrates that the amount of reacted Ni increased with increasing peak temperature in the Sn-37Pb system. Relatively speaking, the rate of Ni consumption increased significantly in the Sn-3.5Ag system. This is attributed to the fact that growth of the $(Ni_{1-x},Cu_x)_3Sn_4$ IMC in the Sn-3.5Ag joints was greater than that in the Sn-37Pb joints. The average

Table III. Thickness of Unconsumed Ni and Average Concentrations of Cu in the Ni Layer and Total Concentration of Cu in the Diffusion Zone in the Solder/UBM Joint during Multiple Reflows

Solder Joint Type	Peak Temperature	Reflow Cycles	Ni Thickness Unconsumed (μm)	Cu Content in Ni Layer (wt.%)	Total Concentration of Cu in Diffusion Zone in Solder (μm•wt.%)
Sn-3.5Ag	260°C	1	3.11 ± 0.13	1.31 ± 0.12	3.39
		4	2.53 ± 0.15	1.45 ± 0.08	3.67
		10	2.16 ± 0.12	1.47 ± 0.11	4.12
Sn-37Pb	245°C	1	3.25 ± 0.10	1.19 ± 0.06	3.64
		3	3.18 ± 0.13	1.22 ± 0.10	3.79
		5	2.97 ± 0.13	1.25 ± 0.11	3.98
		10	2.73 ± 0.17	1.31 ± 0.06	4.28
	265°C	1	3.20 ± 0.18	1.21 ± 0.07	3.69
		3	3.12 ± 0.16	1.24 ± 0.09	3.85
		5	2.90 ± 0.10	1.27 ± 0.09	4.09
		10	2.65 ± 0.12	1.32 ± 0.11	4.31

Cu content in the Ni metallization for the Sn-Ag joint increased from 1.31 wt.% to 1.45 wt.% and 1.47 wt.% for various reflows from one to four and ten times, respectively. Similar phenomena prevailed for the Sn-Pb joint reflowed at both 245°C and 265°C.

The Cu Content in IMCs

Table IV exhibits the thickness of IMCs and average concentration of Cu in IMCs for Sn-3.5Ag and Sn-37Pb solder joints after multiple reflows. The growth of the $(Ni_{1-x},Cu_x)_3Sn_4$ IMC increased gradually with increasing reflows, as displayed in Table IV for the Sn-3.5Ag solder joints. The thickness of the $(Ni_{1-x},Cu_x)_3Sn_4$ IMC in Sn-37Pb solder joints increased gradually with increasing reflows except for that at 265°C for ten reflows. The reduced thickness of the $(Ni_{1-x},Cu_x)_3Sn_4$ IMC in the Sn-Pb joint reflowed at 265°C after ten reflows was due to the fact that some of the $(Ni_{1-x},Cu_x)_3Sn_4$ IMC transformed to the $(Cu_{1-y},Ni_y)_6Sn_5$ IMC.[17]

In the Sn-3.5Ag system, the average concentration of Cu in the $(Ni_{1-x},Cu_x)_3Sn_4$ IMC increased slowly with the reflow cycles. It was 1.20 wt.%, 1.21 wt.%, and 1.29 wt.% for reflows of one, four, and ten cycles, respectively. With increasing reflows in the Sn-37Pb solder joints, the Cu concentration in the $(Ni_{1-x},Cu_x)_3Sn_4$ IMC gradually increased, while that in the $(Cu_{1-y},Ni_y)_6Sn_5$ IMC decreased slightly. In fact, the composition of the $(Ni_{1-x},Cu_x)_3Sn_4$ and $(Cu_{1-y},Ni_y)_6Sn_5$ IMCs were altered and moved toward the equilibrium between Ni_3Sn_4 and Cu_6Sn_5 with increasing reflows.[17]

The Cu Content in the Solder

To obtain the total concentration of Cu in the diffusion zone within the solder, electron microprobe traces were drawn across the interface of the solder/Ni/Cu joint after multiple reflows, as indicated in Figs. 12b, 13b, and 14b. It appears that the Cu content in the solder decreased gradually from the

Table IV. The Type and Thickness of IMC and Average Concentrations of Cu in IMC for Sn-37Pb and Sn-3.5Ag Solder Joints after Multiple Reflows

Solder Joint Type	Peak Temperature	Reflow Cycles	IMC Type	IMC Thickness (μm)	Average Cu Concentration in IMC (wt.%)
Sn-3.5Ag	260°C	1	$(Ni,Cu)_3Sn_4$	0.72 ± 0.25	1.20 ± 0.15
		4	$(Ni,Cu)_3Sn_4$	1.76 ± 0.63	1.21 ± 0.13
		10	$(Ni,Cu)_3Sn_4$	2.58 ± 0.78	1.29 ± 0.15
Sn-37Pb	245°C	1	$(Ni,Cu)_3Sn_4$	0.76 ± 0.06	2.34 ± 0.58
		3	$(Ni,Cu)_3Sn_4$	0.92 ± 0.23	2.34 ± 0.55
		5	$(Ni,Cu)_3Sn_4$	1.11 ± 0.28	4.38 ± 1.16
			$(Cu,Ni)_6Sn_5$	0.49	26.86 ± 2.33
		10	$(Ni,Cu)_3Sn_4$	1.48 ± 0.48	4.67 ± 1.45
			$(Cu,Ni)_6Sn_5$	1.37	26.47 ± 2.12
	265°C	1	$(Ni,Cu)_3Sn_4$	0.77 ± 0.16	2.34 ± 0.58
		3	$(Ni,Cu)_3Sn_4$	0.94 ± 0.30	2.63 ± 1.17
			$(Cu,Ni)_6Sn_5$	0.68	26.86 ± 1.94
		5	$(Ni,Cu)_3Sn_4$	1.08 ± 0.44	4.38 ± 1.16
			$(Cu,Ni)_6Sn_5$	0.69	26.47 ± 1.77
		10	$(Ni,Cu)_3Sn_4$	1.02 ± 0.32	5.54 ± 1.45
			$(Cu,Ni)_6Sn_5$	2.09	25.70 ± 2.33

$(Ni_{1-x},Cu_x)_3Sn_4$/solder interface toward the solder side in all joints. For the sake of simplicity, the total concentration of Cu in the diffusion zone, $C_{Cu\ in\ solder}$, can be expressed as

$$C_{Cu\ in\ solder} = \sum_{j=1}^{n} \frac{1}{2}(c_j + c_{j+1}) \times d \quad (4)$$

where c_j represents the local Cu concentration at the measured point j within the solder, and d is the distance between the adjacent measurement location and is equal 0.5 μm, as indicated in Fig. 12a. It is revealed that the total concentration of Cu in the solder was raised slightly with increasing reflows in all joints, as indicated in Table III. It appears that the Cu atoms that diffused into the solder side in the Sn-3.5Ag joints increased slowly with the reflow cycles. For the Sn-37Pb joints, it is also observed that more Cu atoms diffused into the solders if the reflow temperature was raised.

The Atomic Flux of Cu Diffusion

With the aid of Tables III and IV, the atomic flux of Cu in the Sn-3.5Ag joints reflowed at 260°C and Sn-37Pb joints reflowed at 245°C and 265°C could be determined, as indicated in Fig. 15. The flux of Cu atoms was between 9×10^{16} atoms/cm^{2}sec and 10^{18} atoms/cm^{2}sec and decreased with reflow cycle in both Sn-3.5Ag and Sn-37Pb solder joints. It is clearly exhibited in Fig. 15 that the Cu flux dropped suddenly after one reflow in all joints. However, it decreased rather slowly after three reflows. During one reflow, Cu atoms only diffused through the Ni metallization toward the solder. As a result, a scalloped-type $(Ni_{1-x},Cu_x)_3Sn_4$ IMC formed and covered the Ni metallization. It is argued that the formation of the $(Ni_{1-x},Cu_x)_3Sn_4$ IMC impeded the diffusion of Cu atoms in both Sn-3.5Ag and Sn-37Pb joints. The Cu atoms passed through the $(Ni_{1-x},Cu_x)_3Sn_4$ IMC and then dissolved into the solder. Recently, the ripening flux of Cu in the reaction of eutectic SnPb solder/Cu at 200°C was evaluated between 10^{16} atoms/cm^{2}sec and 10^{17} atoms/cm^{2}sec,[18] about one order of magnitude less than that determined in this study. This is due to the lower annealing temperature of 200°C, as compared to the peak temperature employed in this study.

Figure 16 shows the amount of Cu atoms diffused in the Sn-3.5Ag and Sn-37Pb joints during multiple reflows. The amount of diffused Cu atoms increased gradually with increasing reflow cycle in both the Sn-3.5Ag and Sn-37Pb joints. Besides, the amount of diffused Cu atoms in the Sn-3.5Ag system was less than that in the Sn-37Pb system, as displayed in Fig. 16.

The Effect of Cu Solubility in the Solder on the Formation of the $(Cu_{1-y},Ni_y)_6Sn_5$ IMC

As mentioned before, the flux and amount of Cu atoms diffused through Ni in the Sn-3.5Ag joints were close to that in the Sn-37Pb joints during multiple reflows, as indicated in Figs. 15 and 16. It should be pointed out that no $(Cu_{1-y},Ni_y)_6Sn_5$ IMC was found in the Sn-3.5Ag solder joints even after ten reflows. The different interfacial reactions between Sn-3.5Ag and Sn-37Pb solder joints could be related to the concentration of Cu in the solder adhering to the solder/IMC interface. To explain the Cu distribution near the solder/IMC interface, concentration profiles of Cu along the trace lines both perpendicular and parallel to the interface of the solder/IMC were carried out, as displayed in Figs. 12–14. Because of the formation of the $(Cu_{1-y},Ni_y)_6Sn_5$ IMC in the Sn-37Pb joint reflowed at 245°C after ten reflows, two perpendicular trace lines, i.e., lines 5 and 6, were considered, as indicated in Fig. 14. One passed through the $(Ni_{1-x},Cu_x)_3Sn_4$ and $(Cu_{1-y},Ni_y)_6Sn_5$ IMCs in sequence, and the other was only across the $(Ni_{1-x},Cu_x)_3Sn_4$ IMC.

In the Sn-3.5Ag solder joint after ten reflows, the concentration profiles 1 and 2 in Fig. 12b and c exhibited that the Cu concentration adjacent to the solder/$(Ni_{1-x},Cu_x)_3Sn_4$ interface was less than 0.4 wt.%. In addition, the average concentration of Cu near the solder/$(Ni_{1-x},Cu_x)_3Sn_4$ interface was 0.29 ± 0.06 wt.%, as revealed in Fig. 12c. The concentration

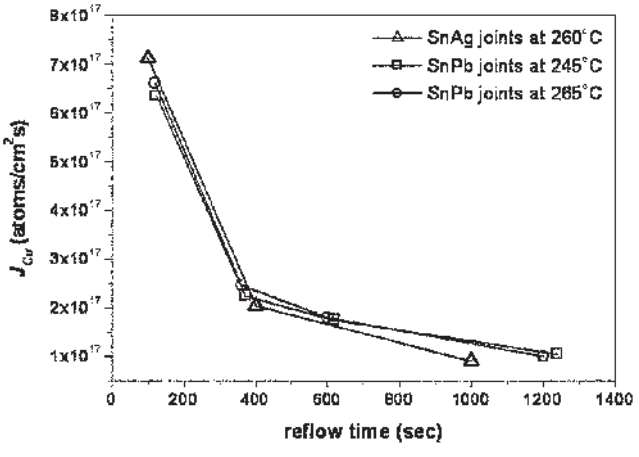

Fig. 15. The atomic flux of Cu in the Sn-3.5Ag and Sn-37Pb solder joints during multiple reflows.

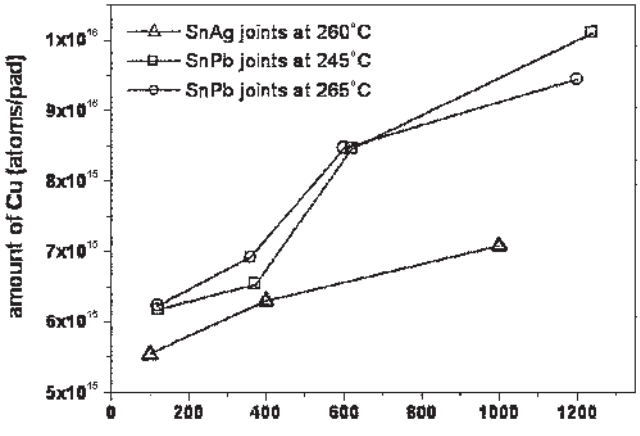

Fig. 16. The amount of Cu atoms diffused in the Sn-3.5Ag and Sn-37Pb solder joints during multiple reflows.

of Cu in the $(Ni_{1-x},Cu_x)_3Sn_4$ IMC decreased gradually from the Ni/IMC side toward the IMC/solder side, as indicated in Fig. 12b.

From the concentration profiles along line 3 in Fig. 13b, it is evident that the concentration of Cu decreased gradually from 0.66 wt.% adjacent to the solder/$(Ni_{1-x},Cu_x)_3Sn_4$ interface down to essentially zero in the Sn-37Pb solder joint reflowed at 245°C for three cycles. The concentration profile along line 3 in Fig. 13c clearly indicated that the concentration of Cu adjacent to the solder/$(Ni_{1-x},Cu_x)_3Sn_4$ interface was in the range of 0.23–0.66 wt.%. In the Sn-37Pb solder joint reflowed at 245°C for ten cycles, the concentration profile passing through the $(Ni_{1-x},Cu_x)_3Sn_4$/solder interface, i.e., trace line 5 in Fig. 14b, showed that the Cu content adjacent to the solder/$(Ni_{1-x},Cu_x)_3Sn_4$ interface was close to 0.8 wt.%, and it then decreased slowly down to zero if far away from the IMC/solder interface. The concentration profile along line 7 in Fig. 14d indicated the average concentration of Cu in the solder near the solder/$(Ni_{1-x},Cu_x)_3Sn_4$ interface was around 0.62 ± 0.19 wt.%. However, it is clearly indicated from the concentration profile along line 6 in Fig. 14c that the Cu concentration adjacent to the $(Cu_{1-y},Ni_y)_6Sn_5$ IMC in the solder was only 0.5 wt.%. In addition, the composition of Cu in the $(Cu_{1-y},Ni_y)_6Sn_5$ IMC was altered in both concentration profiles along lines 6 and 7. This will be further discussed later.

It is evidenced from an enlarged diagram near the Sn corner of the Sn-Cu-Ni ternary isotherm[19–22] that the maximum solubility of Ni and Cu in the Sn-rich phase was less than 0.2 wt.% and 1.1 wt.%, respectively. As a result, when the concentration of Cu in the Sn-Cu-Ni alloy was greater than 0.6 wt.%, the $(Cu_{1-y},Ni_y)_6Sn_5$ IMC might form. On the contrary, only $(Ni_{1-x},Cu_x)_3Sn_4$ would form as the Cu content was less than 0.6 wt.%. Accordingly, no Cu_6Sn_5 IMC was ever observed in the Sn-3.5Ag joint even after ten reflows. The experimentally observed phenomena in this study are in agreement with the information derived from the phase diagram.

Recently, the effect of Cu concentration in Sn-Cu and Sn-Ag-Cu solders on the interfacial reaction between solders and Ni was reported.[23,24] Kao and coworkers claimed that if the Cu concentration was as low as 0.2 wt.%, only $(Ni,Cu)_3Sn_4$ was observed. For a higher concentration of Cu, the interfacial product was $(Cu,Ni)_6Sn_5$, instead. It is apparent that the results in this study through detailed quantitative analysis of the elemental redistribution in the solder joint are in agreement with Kao et al.'s observation.

Phase Equilibrium in the Interface between Solder and UBM

In the Sn-3.5Ag joints, only the $(Ni_{1-x},Cu_x)_3Sn_4$ IMC formed between the solder and the Ni metallization even after ten reflows. This was due to the fact that the concentration of Cu in the solder adjacent to the $(Ni_{1-x},Cu_x)_3Sn_4$ IMC was less than 0.6 wt.%. In the case of ten reflows, the x value in the $(Ni_{1-x},Cu_x)_3Sn_4$ IMC decreased from 0.05 to 0.03 toward the solder, as indicated in Table I and Fig. 1. Thus, the diffusion path in the Sn-3.5Ag solder joint after ten reflows starts in Ni-1.37at.%Cu and passes through $(Ni_{0.94},Cu_{0.05})_3Sn_4$ and $(Ni_{0.97},Cu_{0.03})_3Sn_4$ in sequence, and finally approaches the pure tin phase.

For the Sn-37Pb solder joints reflowed at 245°C for one and three cycles, the composition of the $(Ni_{1-x},Cu_x)_3Sn_4$ IMC was homogeneous in both joints, and the x value was equal to 0.08 (Table II). Nevertheless, the composition variations in the $(Ni_{1-x},Cu_x)_3Sn_4$ IMC were detected after more than five reflows. It is interesting to point out that the minimum values of x in the Sn-37Pb joints reflowed at 245°C for five and ten cycles is identical to that after less than three reflows. On the other hand, the maximum value of x in the Sn-37Pb joints reflowed at 245°C after more than five cycles maintained 0.22 (Table II). It is argued that the maximum solubility of Cu in Ni_3Sn_4 at 245°C is reached, and thus, $(Ni_{0.78},Cu_{0.22})_3Sn_4$ is formed. As to the other IMC, i.e., $(Cu_{1-y},Ni_y)_6Sn_5$, the value of y varied between 0.25 and 0.43 in the Sn-37Pb joints reflowed at 245°C after more than five cycles. Accordingly, the maximum solubility of Ni at 245°C in Cu_6Sn_5 should approach 23.5 at.%, and the $(Cu_{0.57}, Ni_{0.43})_6Sn_5$ IMC is thus revealed. In the Sn-37Pb solder joints reflowed at 265°C after more than three cycles, the x value in the $(Ni_{1-x},Cu_x)_3Sn_4$ IMC altered between 0.08 and 0.24, and the value of y in the $(Cu_{1-y},Ni_y)_6Sn_5$ IMC was between 0.31–0.48 (Table II). Thus, the maximum solubility of Cu in Ni_3Sn_4 should approach 10.3 at.%, and the maximum solubility of Ni in Cu_6Sn_5 is 26.2 at.% at 265°C. The $(Ni_{0.76},Cu_{0.24})_3Sn_4$ and $(Cu_{0.52},Ni_{0.48})_6Sn_5$ IMCs are thus revealed at 265°C.

A parallel study[17] has demonstrated that if the Cu concentration in the Sn-37Pb solder side adjacent to the solder/$(Ni_{1-x},Cu_x)_3Sn_4$ interface is greater than 0.6 wt.%, the $(Ni_{1-x},Cu_x)_3Sn_4$ IMC should transform into the $(Cu_{1-y},Ni_y)_6Sn_5$ IMC. In order to equilibrate with the $(Cu_{1-y},Ni_y)_6Sn_5$ IMC, the Cu content in $(Ni_{1-x},Cu_x)_3Sn_4$ increases gradually until it reaches the maximum solubility of Cu in Ni_3Sn_4. In addition, the concentration of Ni in the as-formed $(Cu_{1-y},Ni_y)_6Sn_5$ IMC is the maximum solubility of Ni in Cu_6Sn_5. To be equilibrated with the solder, the Ni solubility in the $(Cu_{1-y},Ni_y)_6Sn_5$ IMC decreases gradually from the maximum solubility near the $(Ni_{1-x},Cu_x)_3Sn_4$ IMC to the adjacent solder. Thus, there are two diffusion paths between $(Ni_{1-x},Cu_x)_3Sn_4$ and $(Cu_{1-y},Ni_y)_6Sn_5$ IMCs for the Sn-37Pb system in this study. One should be from $(Ni_{0.92},Cu_{0.08})_3Sn_4$ through $(Ni_{0.78},Cu_{0.22})_3Sn_4$ and $(Cu_{0.57},Ni_{0.43})_6Sn_5$ and then arrive at $(Cu_{0.75},Ni_{0.25})_6Sn_5$ in the joints reflowed at 245°C. The other one for the joints reflowed at 265°C originates in $(Ni_{0.92},Cu_{0.08})_3Sn_4$ and then passes through $(Ni_{0.76},Cu_{0.24})_3Sn_4$ and $(Cu_{0.52},Ni_{0.48})_6Sn_5$ in sequence, and finally reaches $(Cu_{0.69},Ni_{0.31})_6Sn_5$.

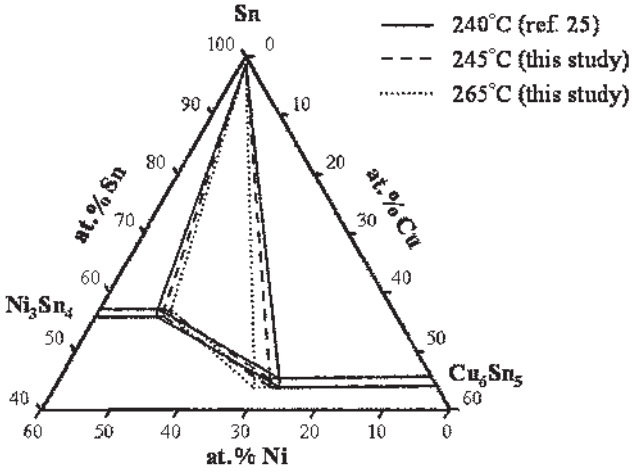

Fig. 17. The Sn-Ni_3Sn_4-Cu_6Sn_5 ternary-phase region at 240°C,[25] 245°C, and 265°C in the Sn-Ni-Cu ternary-phase isotherm.

Another parallel study concerning the Sn-Cu-Ni ternary isotherm at 240°C has been investigated.[25] Li and Duh reported that the maximum solubility of Cu in the Ni_3Sn_4 IMC was very close to 9.2 at.%, and the maximum solubility of Ni in the Cu_6Sn_5 IMC approached 22.4 at.%. In combination with data in this study, an enlarged Sn corner of the Sn-Cu-Ni ternary isotherm was proposed at 240°C, 245°C, and 265°C, respectively, as shown in Fig. 17. It is clearly indicated from Fig. 17 that the maximum solubility of both Cu in Ni_3Sn_4 and Ni in Cu_6Sn_5 increases with increasing temperature. Thus, with increasing temperature, the tie line at maximum solubility of Cu in Ni_3Sn_4 shifts rightward and that at maximum solubility of Ni in Cu_6Sn_5 moves leftward.

CONCLUSIONS

Only the $(Ni_{1-x},Cu_x)_3Sn_4$ IMC formed between the solder and the Ni metallization in the Sn-3.5Ag/Ni/Cu solder joints after one to ten reflows. This is attributed to fact that the Cu concentration in the solder adjacent to the $(Ni_{1-x},Cu_x)_3Sn_4$ IMC was less than 0.6 wt.%. In addition, the atomic flux of Cu diffusion during reflow was on the order of 10^{16}–10^{17} atoms/cm^2sec in Sn-3.5Ag solder joints and decreased with increasing reflows.

In the Sn-37Pb/Ni/Cu joints reflowed at 225°C, only the $(Ni_{1-x},Cu_x)_3Sn_4$ IMC formed between the solder and the Ni layer even after ten reflows. If reflowed at 245°C after one and three cycles, there was only the $(Ni_{1-x},Cu_x)_3Sn_4$ IMC formed at the solder/Ni interface. If the concentration of Cu in the solder near the $(Ni_{1-x},Cu_x)_3Sn_4$ IMC was greater than 0.6 wt.%, the $(Ni_{1-x},Cu_x)_3Sn_4$ IMC transformed into the $(Cu_{1-y},Ni_y)_6Sn_5$ IMC as in case of the Sn-37Pb joints reflowed at 245°C after more than five cycles. Besides, the Cu content in the solder for the Sn-37Pb solder joint reflowed at 265°C after three cycles was larger than 0.6 wt.%. Consequently, the $(Cu_{1-y},Ni_y)_6Sn_5$ IMC was revealed in addition to the $(Ni_{1-x},Cu_x)_3Sn_4$ IMC. As a result, the amount of diffused Cu atoms in the solder could be altered by modifying the peak temperature of reflow in the Sn-37Pb solder joints, and thus, the formation of the $(Cu_{1-y},Ni_y)_6Sn_5$ IMC could be controlled.

ACKNOWLEDGEMENTS

The financial support and joint assemblies preparation from Taiwan Semiconductor Manufacturing Company are acknowledged. Partial support from the National Science Council under the Contract No. NSC-92-2216-E007-037 is also appreciated.

REFERENCES

1. K.S. Bae and S.J. Kim, *J. Mater. Res.* 17, 743 (2002).
2. H.W. Miao and J.G. Duh, *Mater. Chem. Phys.* 71, 255 (2001).
3. D.R. Frear, J.W. Jang, J.K. Lin, and C. Zang, *JOM* 53, 28 (2001)
4. B.L. Young, J.G. Duh, and B.S. Chiou, *J. Electron. Mater.* 30, 543 (2001).
5. M. McCormack, S. Jin, G.W. Kammlott, and H.S .Chen, *Appl. Phys. Lett.* 63, 15 (1993).
6. L.F. Miller, *IBM J. Res. Development* 13, 239 (1969).
7. J.H. Lau, *Flip Chip Technologies* (New York: McGraw-Hill, 1996), pp. 26–30.
8. G.R. Blackwell, *The Electronic Packaging Handbook* (Boca Raton, FL: CRC Press, 2000), pp. 4.4–4.25.
9. A.A. Liu, H.K. Kim, K.N. Tu, and P.A. Totta, *J. Appl. Phys.* 80, 2774 (1996).
10. D.R. Frear, F.M. Hosking, and P.T. Vianco, *Materials Developments in Microelectronic Packaging Conf. Proc.* (Materials Park, OH: ASM International, 1991), pp. 229–240.
11. R.G. Werner, D.R. Frear, J. DeRosa, and E. Sorongon, *1999 Int. Symp. on Advanced Packaging Materials* (Reston, VA: IMAPS; Piscataway, NJ: IEEE, 1999), pp. 246–251.
12. C.S. Huang, J.G. Duh, Y.M. Chen, and J.H. Wang, *J. Electron. Mater.* 32, 89 (2003).
13. C.S. Huang, J.G. Duh, and Y.M. Chen, *J. Electron. Mater.* 32, 1509 (2003).
14. C.S. Huang and J.G. Duh, *J. Mater. Res.* 18, 935 (2003).
15. C.S. Huang, G.Y. Jang, and J.G. Duh, *J. Electron. Mater.* 33, 283 (2004).
16. J.I. Goldstein, *Scanning Electron Microscopy and X-ray Microanalysis* (New York: Plenum Press, 1992), pp. 306–330.
17. G.Y. Jang, C.S. Huang, L.Y. Hsiao, J.G. Duh, and H. Takahashi, *J. Electron Mater.* 33, 1118 (2004).
18. H.K. Kim and K.N. Tu, *Phys. Rev. B* 53, 16027 (1996).
19. C.H. Lin, S.W. Chen, and C.H. Wang, *J. Electron. Mater.* 31, 907 (2002).
20. K.N. Tu and K. Zeng, *Mater. Sci. Eng. R* 34, 1 (2001).
21. M. Li, F. Zhang, W.T. Chen, K. Zeng, K.N. Tu, H. Balkan, and P. Elenius, *J. Mater. Res.* 17, 1612 (2002).
22. K. Zeng, V. Vuorinen, and J.K. Kivilahti, *Proc. 51st Electronic Components and Technology Conf.* (Piscataway, NJ: IEEE, 2001), pp. 693–698.
23. C.E. Ho, R.Y. Tsai, Y.L. Lin, and C.R. Kao, *J. Electron. Mater.* 31, 584 (2002).
24. W.T. Chen, C.E. Ho, and C.R. Kao, *J. Mater. Res.* 17, 263 (2002).
25. C.Y. Li and J.G. Duh, submitted to *J. Mater. Res.*